Case Studies in Structural Engineering 3 (2015) 33–51

Contents lists available at ScienceDirect

Case Studies in Structural Engineering

journal homepage: www.elsevier.com/locate/csse

Analytical study on new types of reduced beam section moment connections affecting cyclic behavior

R. Rahnavard [a,*], A. Hassanipour [b,1], N. Siahpolo [a,2]

[a] Dep. of Civil Engineering, Institute for Higher Education ACECR Khouzestan, Ahvaz, Khouzestan State, Iran
[b] Dep. of Civil Engineering, Jondi Shapour University of Dezful, Dezful, Khouzestan State, Iran

ARTICLE INFO

Article history:
Available online 2 April 2015

Keywords:
RBS connections
Cyclic behavior
Ductility
Panel zone
PEEQ

ABSTRACT

Recent earthquakes have shown that steel moment frame (SMF) with weld connections are so brittle. According to the studies conducted, great damages are due to the cracking of the weld between the beam flange and the column face and inducing concentrated stresses in this area. A useful approach to reduce the stress concentration at the panel zone could be the use of reduced beam section (RBS). Given the enormous impact of seismic behavior and ductility of the panel zone, RBS moves plastic hinge formation at an appropriate distance from column face. In this study, eight moment connections with different shape of reducing beam flange have been modeled using ABAQUS computer program and compared with each other during cyclic behavior. The obtained result of this study showed that using varied holes, reduced beam section is more ductile and will dissipate energy more than other connections.

Introduction

Since 1994 Northridge earthquake, a bulk of research have been performed to replace better connections for new steel moment frame and to enrich poor moment connections for exiting steel moment frames. The prior and post-Northridge laboratory observations have also demonstrated the inherent disability of the conventional moment connections to develop enough ductility (Calado, 2000) [1].

Since the Northridge earthquake, a number of various studies have been carried out in order to improve the seismic performance of the conventional welded connections. One of the most promising ways to modify the behavior of the conventional moment frame is to soften a portion of beam flanges near the column face (Plumier, 1997, Engelhard et al. 1998, Yu et al. 1999, Yu and Yang 2001) [2]. The connection softening may be accomplished by trimming circular selectors from the beam flanges near the column. This solution known as reduced beam section (RBS) method, leads plastic hinges toward the beam span away from column face, resulting in the reduction of stress concentration at the interface of beam and column. However, as the result of reducing beam section within a sensitive zone, the beam becomes more prone to buckling. Some studies have been conducted to assess key issues influencing the instability of RBS beams (Deylami and Moslehi Tabar 2008) [3]. Deylami and Moslehi Tabar (2008) [3] defined a new lateral slenderness parameter, which is in good agreement with the experimental data. According to their definition, the cyclic behavior of RBS beams is mostly affected by their lateral instability and the beam depth-to-length ratio. Column panel zone flexibility is another issue affecting the behavior of RBS

* Corresponding author. Mobile: +98 9384723905.
E-mail addresses: Rahnavard1990@gmail.com (R. Rahnavard), hassanipour@gmail.com (A. Hassanipour), N_Siahpolo@mjdkh.ac.ir (N. Siahpolo).
[1] Mobile: +98 9161424718.
[2] Mobile: +98 9161111501.

http://dx.doi.org/10.1016/j.csse.2015.03.001
2214-3998/

connections. Tsai and Chen (2002) and Jones et al. (2002) experimentally illustrated that RBS moment connections with moderately strong panel zones show appropriate performance. Sang-Whan Han, Ki-Hoon Moon and Bozidar Stojadinovic (2009, 2010) [4,5] studied the design equations of RBS connections and found that RBS-B connection moment strength equation specified in FEMA-350, consistently overestimates the actual strength of the RBS-B connections measured in tests and the reduction of beam sections according to FEMA-350 which may therefore be insufficient to protect the RBS-B connections. This, in turn, may lead to RBS-B connection failure before a plastic hinge forms at the reduced beam section of the beam. Rahnavard and Siahpolo (2013) [6] studied bolt and weld moment connections in both with and without reduced section. They made some models in ABAQUS software and compared them to find that the RBS connections would increase ductility of beam and panel zone and also would result in the reduction of stress and plastic strain concentration at the interface of beam and column. Moslehi Tabar and Deylami (2013) [7] considered a new detail and proposed that the RBS performance be enhanced by delaying beam buckling. The efficiency of the proposed detail was investigated by a large scale laboratory testing under cyclic loading. The results of their study showed that the proposed RBS connection had superior performance as

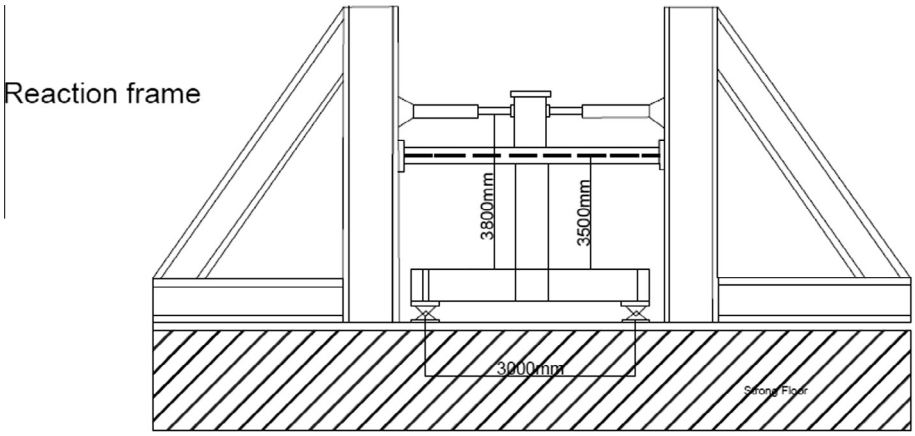

Fig. 1. The specifications of specimens and test set-up.

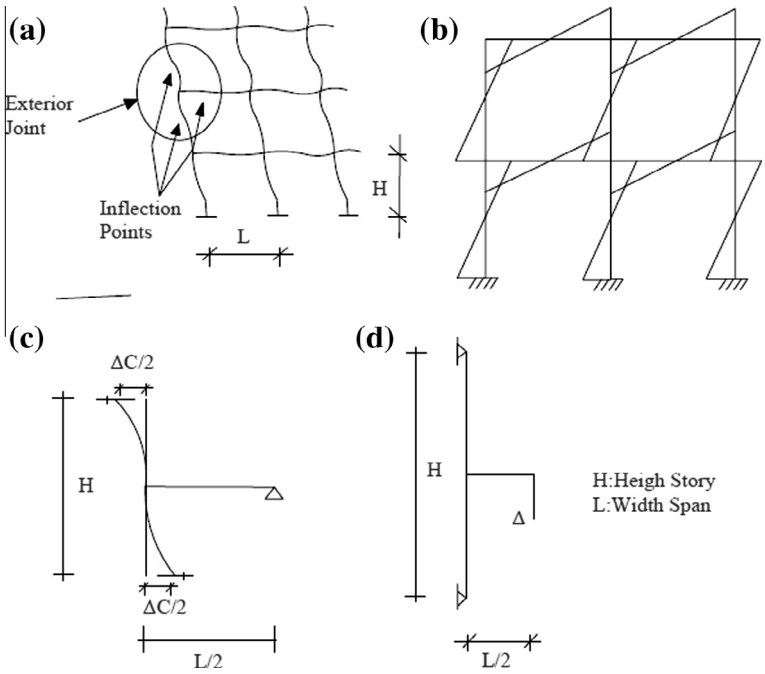

Fig. 2. (a) Deflection diagram of the moment resisting frame, (b) Moment diagram, (c) Exterior connection separated from inflection point, (d) Applied substructure in numerical study.

compared with the conventional one. The proposed detail increased plastic rotation capacity of the conventional RBS connection.

The present paper aims to obtain results of numerical modeling on eight subassemblies RBS moment connections. The main objectives include: (1) to make comparison between all type of RBS connection on ductility; (2) to study the effect of all types of reduced beam connection on concentration stress, strain and equivalent plastic strain at integration point (PEEQ) in different zones; (3) to obtain the influence of various types of reduced flange section on dissipated energy by the whole model; (4) to consider the buckling behavior of the exterior models.

Numerical study of RBS connection

The analytical study involves developing finite element model of connections for the purpose of evaluating the effect of various parameters on connection behavior. Three–dimensional nonlinear finite element of 8 models were created using

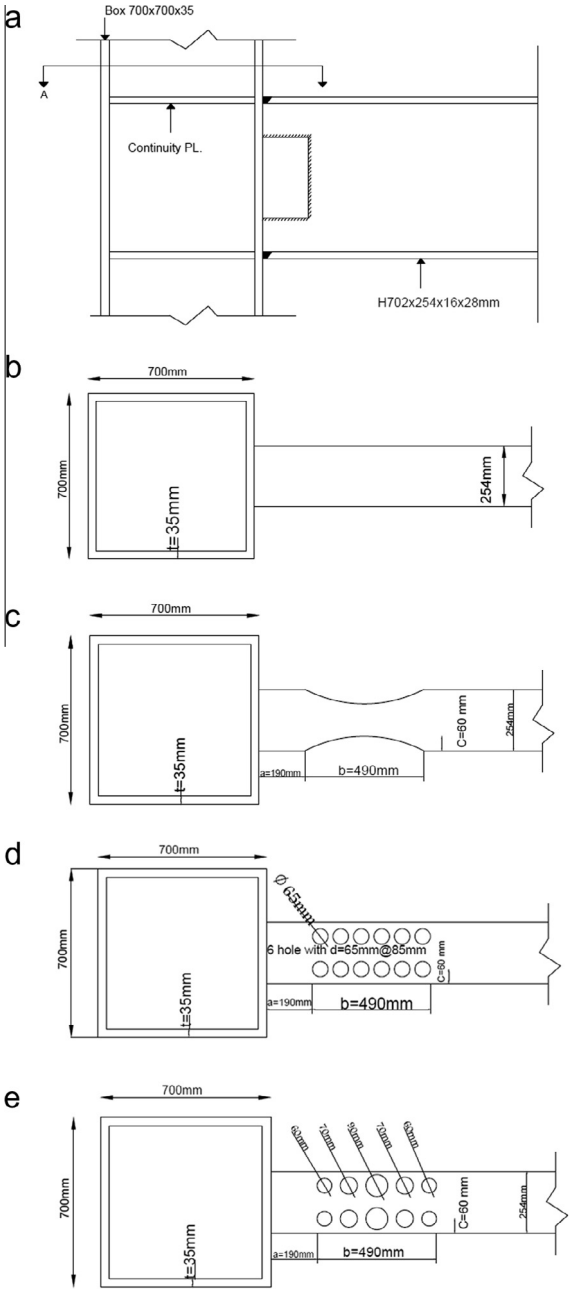

Fig. 3. The details of connections. (a) Connection side view, (b) ORC, (c) RBS, (d) RBS2-SH and (e) RBS1-VH.

ABAQUS computer program. The geometry and boundary conditions of the simple connection were based on the test set up used in the experimental study (Chou C.C., Kai Y.C., 2010) [8] that are shown on Fig. 1. Point-wise boundary conditions (a pin and a roller) were modeled using rigid plates (un-deformable mesh regions) which were attached to both ends of the column. Lateral movement of the flanges of the beam was prevented from column face in the 3.5 m. Fig. 2 shown the bending moment diagram and deflection of a moment resisting frame under lateral loads. As it can be seen, the bending moment at the mid span of the beam and the column is zero and the midpoint of the beam and the column under lateral loads is the inflection point but the value of the shear force at the inflection point is not zero. Since the frame finite element modeling is very difficult, to considering the behavior of the moment resisting connections it can be investigate separately from the inflection point. The pinned or roller supports can be applied to carry the shear forces at these.

The beam flanges reduced by two methods including radial cutting and circular cutting. The circles of three of the models were the same and three of them increased gradually. Fig. 3 shows four types of the analytical models. Moreover, the analysis for the finite element parametric study considering 8 models, are summarized in Table 1. Grade 50 steel ASTM-572 was used

Table 1
General specifications of the models.

Material	Application	Stress (Mpa)	Strain
ASTM-A572-Gr50	Column, stiffness, shear plate	391	0.02
		525	0.06
		470	0.12
		391	0.24
ASTM-A36	Beam	288	0.013
		495	0.06
		390	0.12
		288	0.24
ER70S-6	Weld	469	0.025
		563	0.125
		510	0.245
		469	0.36

Table 2
Material properties used in FE modeling.

Models	Beam	Column	H (mm)	L_b (mm)	L_0 (mm)	Reduce parameters (mm)
ORC	H 702 × 254 × 16 × 28	Box 700 × 700 × 35	3000	3800	3500	–
RBS	H 702 × 254 × 16 × 28	Box 700 × 700 × 35	3000	3800	3500	a = 190 b = 490 c = 60
RBS1-SH	H 702 × 254 × 16 × 28	Box 700 × 700 × 35	3000	3800	3500	Five circle with d = 70@105 on right and left
RBS2-SH	H 702 × 254 × 16 × 28	Box 700 × 700 × 35	3000	3800	3500	Six circle with d = 65@85 on right and left
RBS3-SH	H 702 × 254 × 16 × 28	Box 700 × 700 × 35	3000	3800	3500	Seven circle with d = 60@71 on right and left
RBS1-VH	H 702 × 254 × 16 × 28	Box 700 × 700 × 35	3000	3800	3500	Five circle that increase gradually d = 60 & 70 & 90 & 70 & 60 on right and left
RBS2-VH	H 702 × 254 × 16 × 28	Box 700 × 700 × 35	3000	3800	3500	Six circle that increase gradually d = 50 & 60 & 80 & 80 & 60 & 50 on right and left
RBS3-VH	H 702 × 254 × 16 × 28	Box 700 × 700 × 35	3000	3800	3500	Seven circle that increase gradually d = 40 & 50 & 70 & 85 & 70 & 50 & 40 on right and left

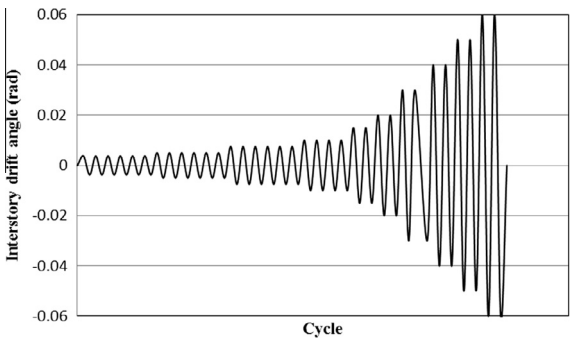

Fig. 4. SAC loading protocol.

for column and continuity plates and ASTM-A36 and ER-70S-6 were also used for beam and weld electrode, respectively. The mechanical properties of all component materials are taken from the experimental specimens mentioned in Table 2. An combined (isotropic–linear kinematic) hardening rule with a Von Mises yielding criterion is applied to simulate the plastic deformations of the connection components. This is suitable for simulation of metal plasticity under cyclic loading [16].

Tie constraint used to define the interactions between weld-beam, weld-column and shear plate-beam web. A displacement-control loading was applied on the tip of the beam by imposing cyclic displacement based on SAC loading protocol (Fig. 4). The beam tip displacement corresponding to the inter story drift angle of 0.01 rad was 38 mm.

A typical three-dimensional finite element model of conventional connection is shown in Fig. 5, where the models composed of eight-node brick elements with standard integration (element C3D8 in the ABAQUS element library). This element had 8 nodes and three degrees of freedom per node. With three elements through the thickness of column flanges and 5 elements and 6 elements used through the beam flanges and beam web, respectively. A better mesh was used to model the connection region and the beam and column region in the vicinity of the connected area.

To verify the analytical models, we modeled the conventional connection (model 1) tested by Chou C.C and Kai Y.C. As shown in Fig. 6, there is a close agreement between the experimental results obtained by Chou C.C and Kai Y.C. and our numerical results. It can be seen from the figure that the maximum moment at the surface between beam and column for experimental specimens and finite element model are 2210 kN.m and 2250 kN.m, respectively; which shows 2% differences in maximum values. Also the moment corresponding 4% radian connection rotate, for experimental and numerical result are 1650 kN.m and 1740 kN.m respectively which shows 6.5% differences.

The comparison between the test and finite element analysis indicates that the finite element modeling procedures produce an accurate model, which should lead to accurate response prediction in the parametric study.

Description of model analysis

Stress distribution

The Von Mises stress distributions for 0.06 rad inter story drift angle are shown in Fig. 6 for all models. It can be seen that concentrated stress for all types of RBS models occurs in beams and for ordinary rigid connection (ORC) occurs in connection. In spite of the fact that in all RBS models, the panel zone remained elastic, in ORC connection the panel zone had nonlinear behavior. As it can be seen, the local buckling of beam flange and web has occurred in 0.06 rad inter story drift. As indicated in Fig. 7, the brittle cracking may happen on weld area on ORC connection during the cyclic load.

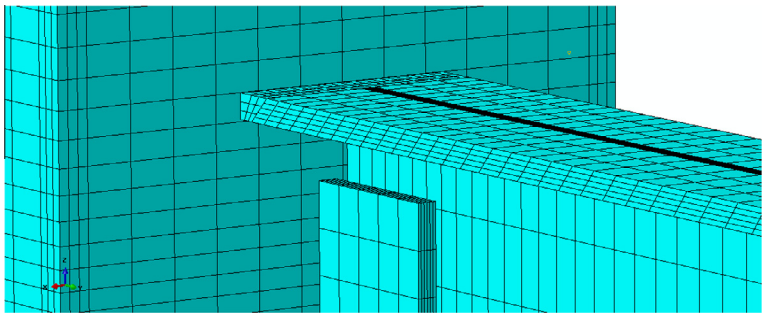

Fig. 5. Finite element model.

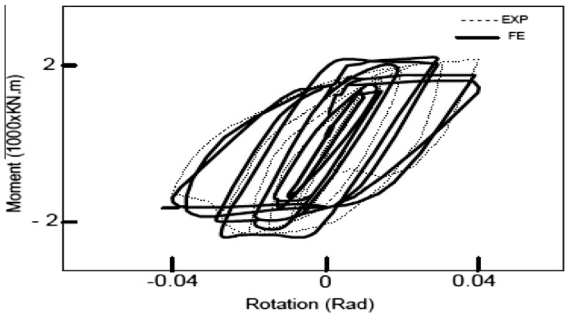

Fig. 6. Comparison between the experimental and numerical hysteretic results.

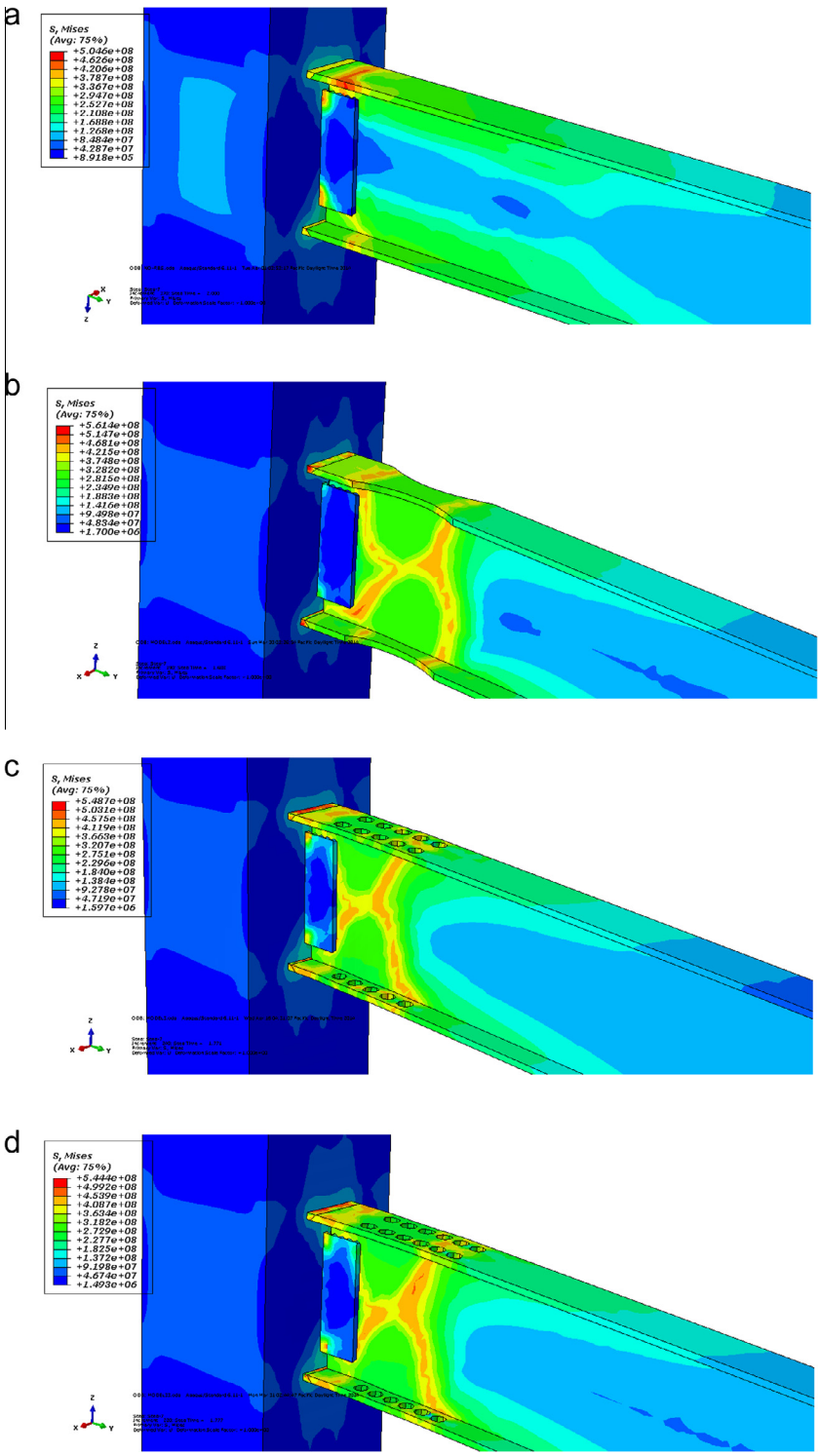

Fig. 7. Von Mises distribution (a) ORC, (b) RBS, (c) RBS1-SH, (d) RBS2-SH, (e) RBS3-SH, (f) RBS1-VH, (g) RBS2-VH, (h) RBS3-VH.

PEEQ

The PEEQ index is defined as the plastic equivalent strain (PEEQ) divided by the yield strain ε_y of the beam material, which represents the local strain demand [9]. The plastic equivalent strain is defined as:

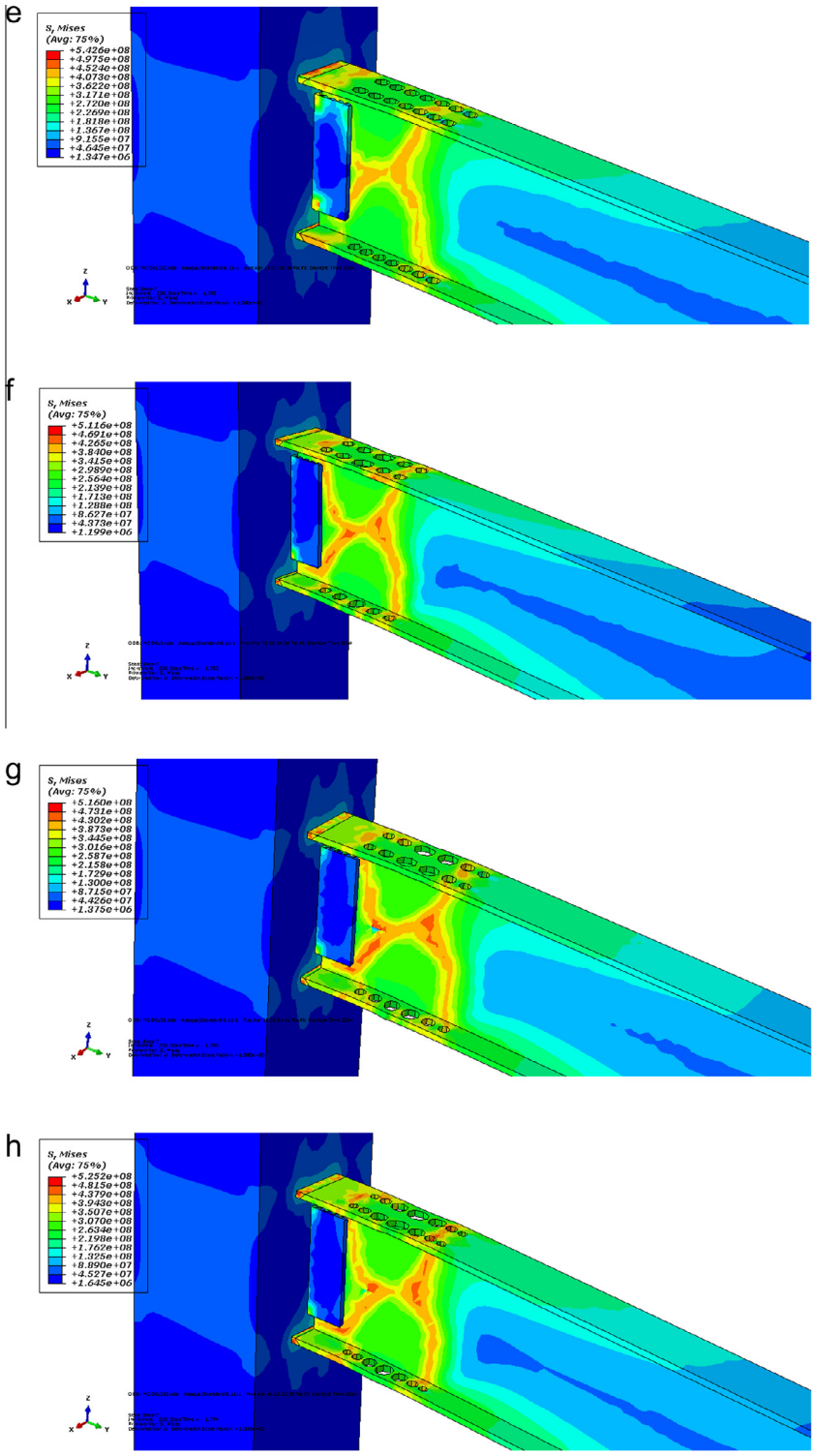

Fig. 7 (*continued*)

$$\mathrm{PEEQ} = \sqrt{\frac{2}{3}\varepsilon_{ij}\varepsilon_{ij}}$$

where ε_{ij} is the component of plastic strain in the direction specified by i and j.

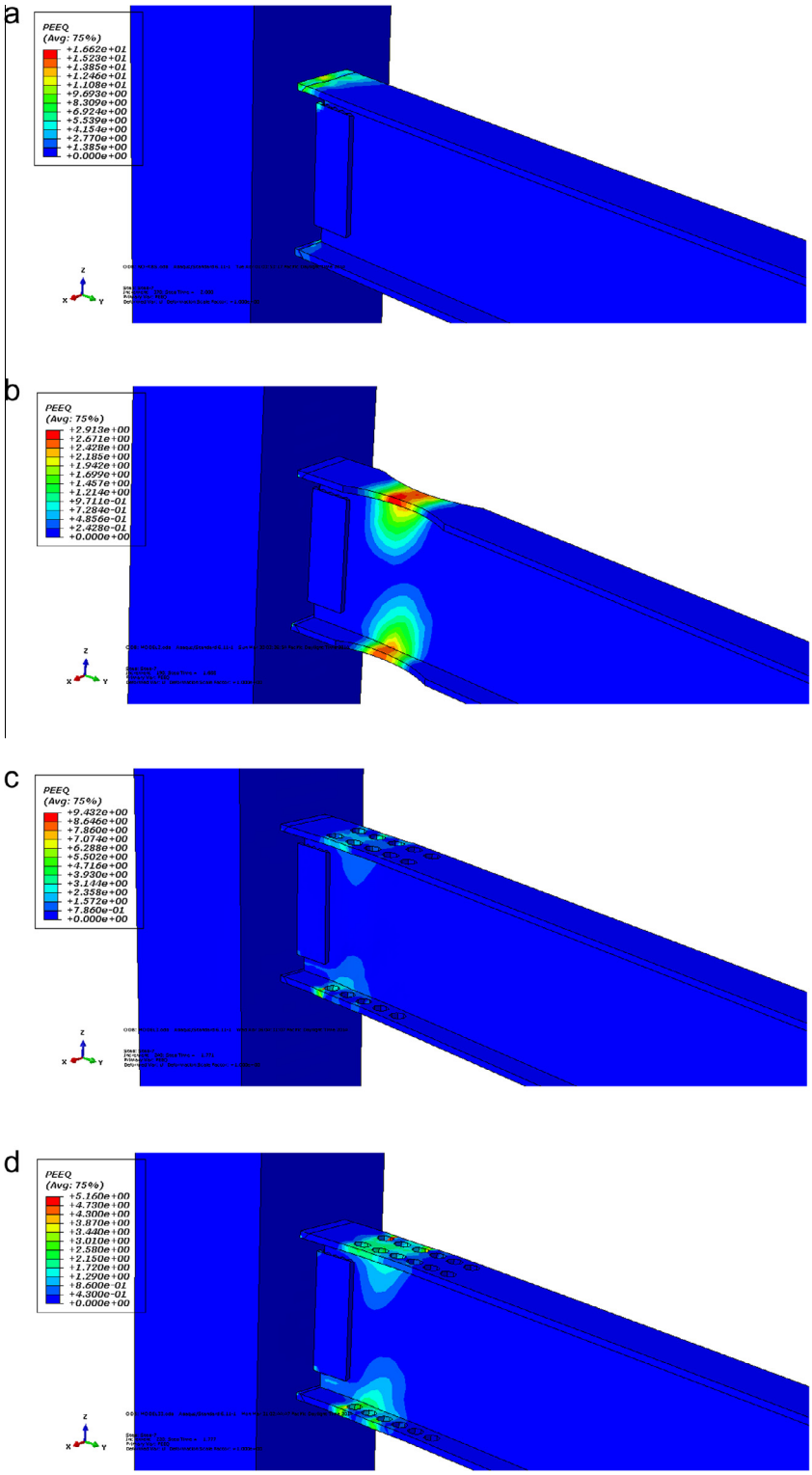

Fig. 8. PEEQ index (a) ORC (b) RBS, (c) RBS1-SH, (d) RBS2-SH, (e) RBS3-SH, (f) RBS1-VH, (g) RBS2-VH, (h) RBS3-VH.

The plastic equivalent strain (PEEQ) distributions for 0.06 rad inter story drift angle are shown in Fig. 8 for all models. It can be seen that concentrated strain for all types of RBS models occurs in beams and for ordinary rigid connection (ORC), it occurs in connection. As indicated in Fig. 8, the plastic hinge occurs in weld groove between beam and column surface for ORC model. As it is evident, all types of reduced beam section moment connections translate plastic hinge from the connection to the beam.

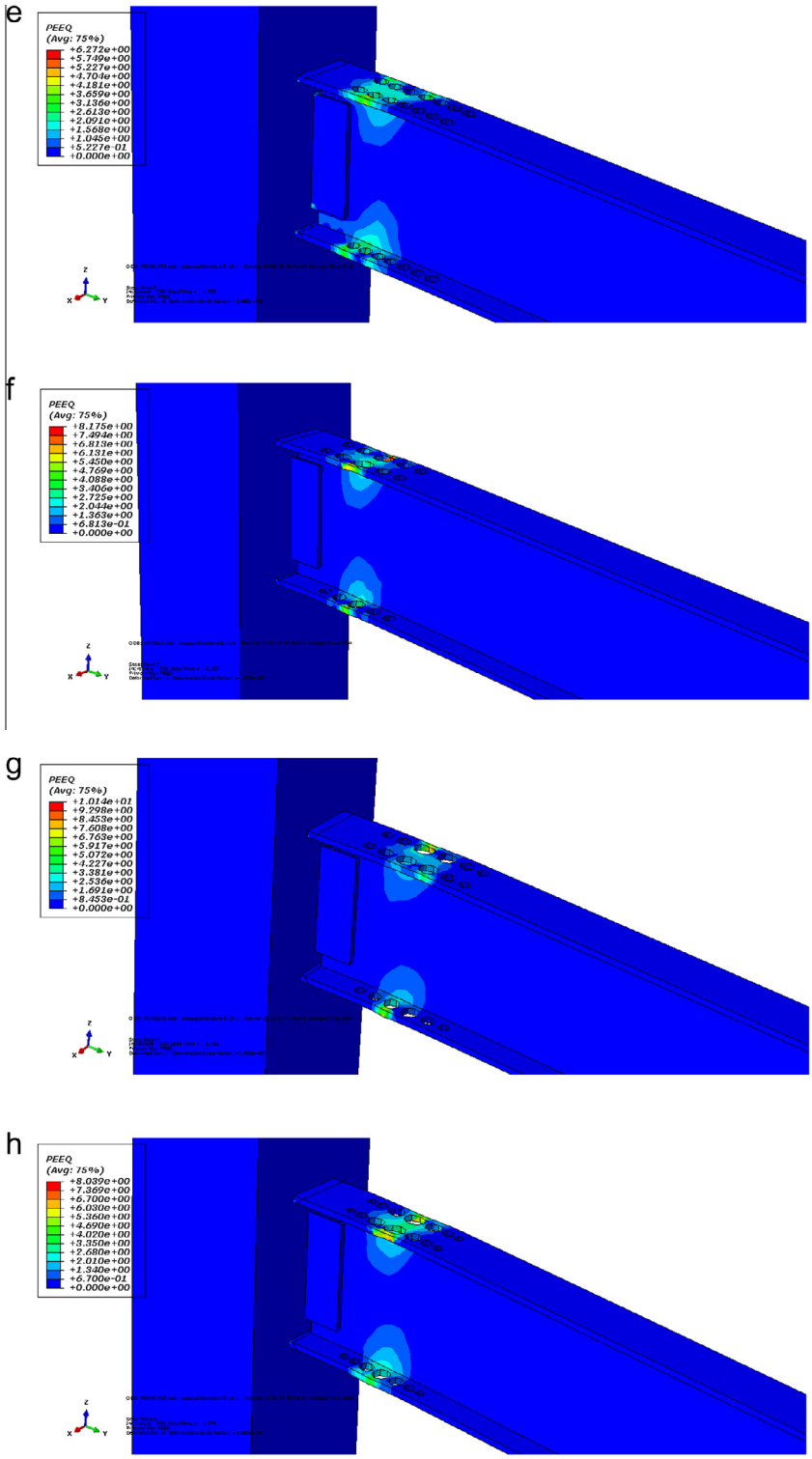

Fig. 8 (*continued*)

To access the effect of the parameters on the ductile fracture potential of the models of the various connection configurations, the Rupture Index (RI) was computed from the finite element analysis results. The RI is defined as the ratio of the equivalent plastic strain (PEEQ) index to the ductile fracture strain ε_f, multiplied by the material constant α i.e.

$$RI = \alpha \frac{\mathrm{PEEQ}/\varepsilon_y}{\varepsilon_f} = \frac{\mathrm{PEEQ}/\varepsilon_f}{\exp\left(1.5\frac{p}{q}\right)}$$

Where p and q are equal to the hydrostatic pressure and Von Mises stress, respectively, with:

$$p = -\frac{1}{3}\sigma_{ii}$$

$$q = \sqrt{\frac{3}{2}S_{ij}S_{ij}}$$

Values of the *RI* were used to evaluate and compare the potential for ductile fracture of different locations in a finite element model or between two different models at the same location. Research by Hancock and Makenzie [10] has shown that this criterion for evaluating the potential for ductile fracture to be accurate. Fig. 9 indicates that the reduced beam section connection (RBS) has a lower RI, and thus fracture potential, compared to ordinary rigid connection (ORC) to a similar condition. The cause for the higher value of the RI in the ORC connection is due to the larger plastic strains that develop in the connection region near the column face. The maximum moment in the beam at the column face is smaller in the RBS connection than the ORC connection, where the latter has a considerable amount of strain hardening in the beam plastic hinge region. For most cases, the largest fracture potential is at the end of the beam web to – column flange CJP groove weld. The larger value for the RI at this location and at the beam flange CJP groove weld is associated with a greater amount of local larger plastic strain that develops at these locations compared to the other cases. As it can be seen in Fig. 9 the RBS3-VH has minimum value of RI to compare with other connection.

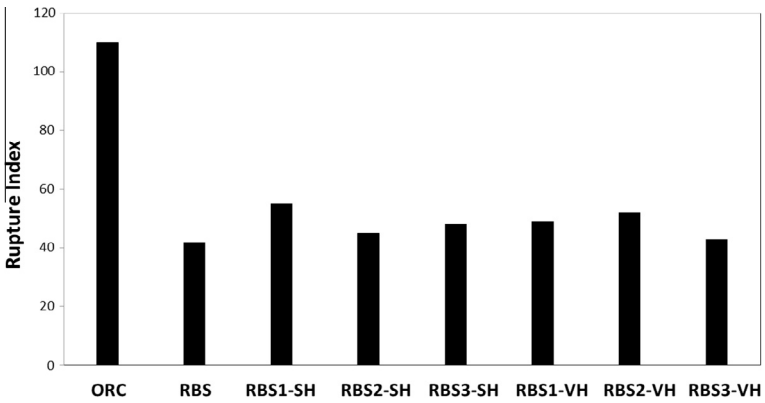

Fig. 9. Effect of reduced type on Rupture Index.

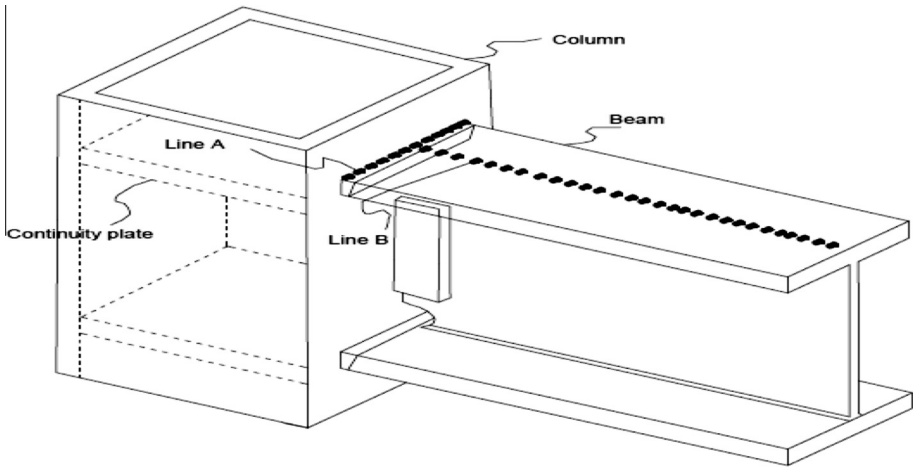

Fig. 10. Critical section.

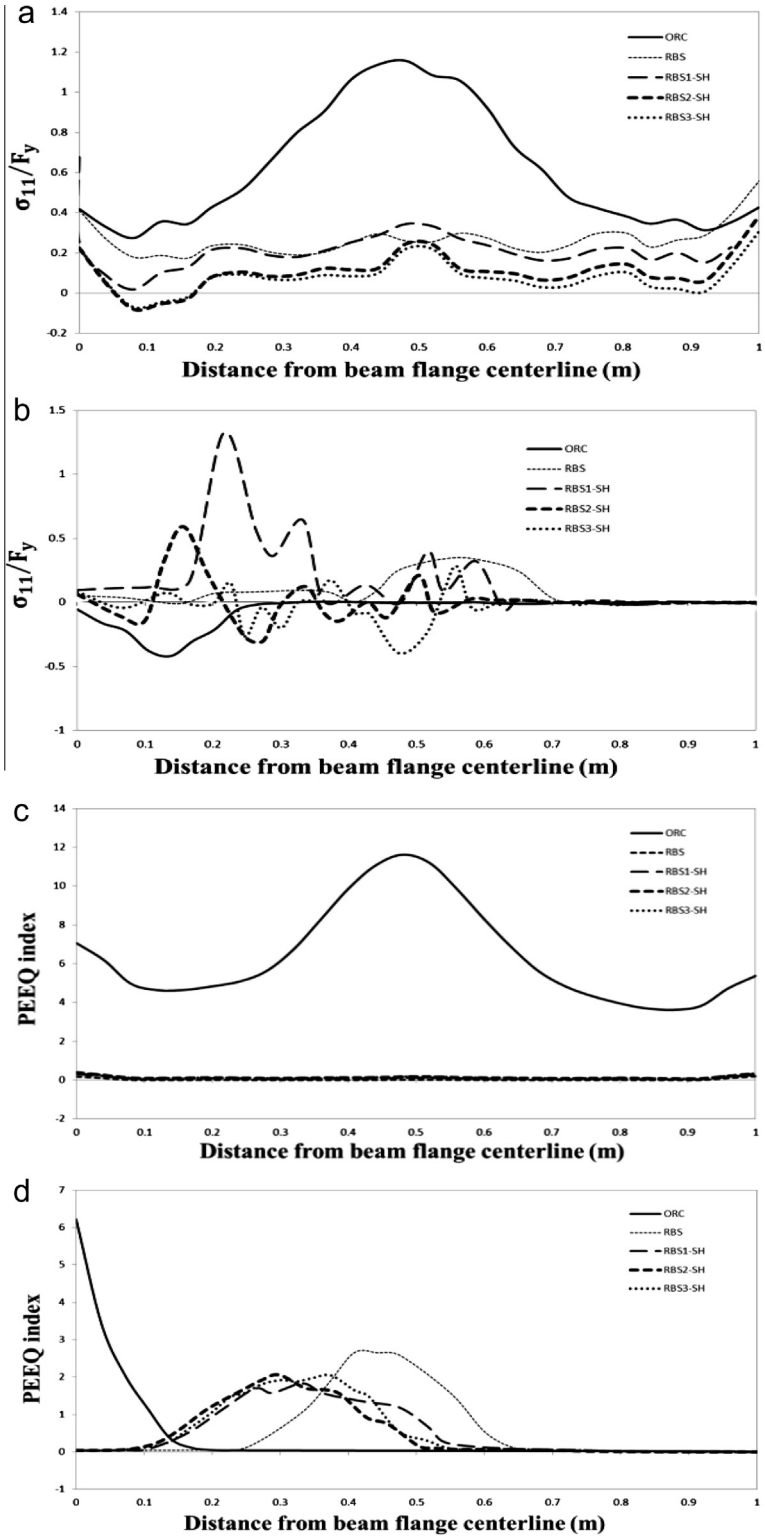

Fig. 11. Longitudinal stresses and PEEQ indices at 0.06 rad rotation for ORC, RBS and RBS-SH: (a) longitudinal stresses along Line A; (b) longitudinal stresses along Line B; (c) PEEQ indices along Line A; (d) PEEQ indices along Line B.

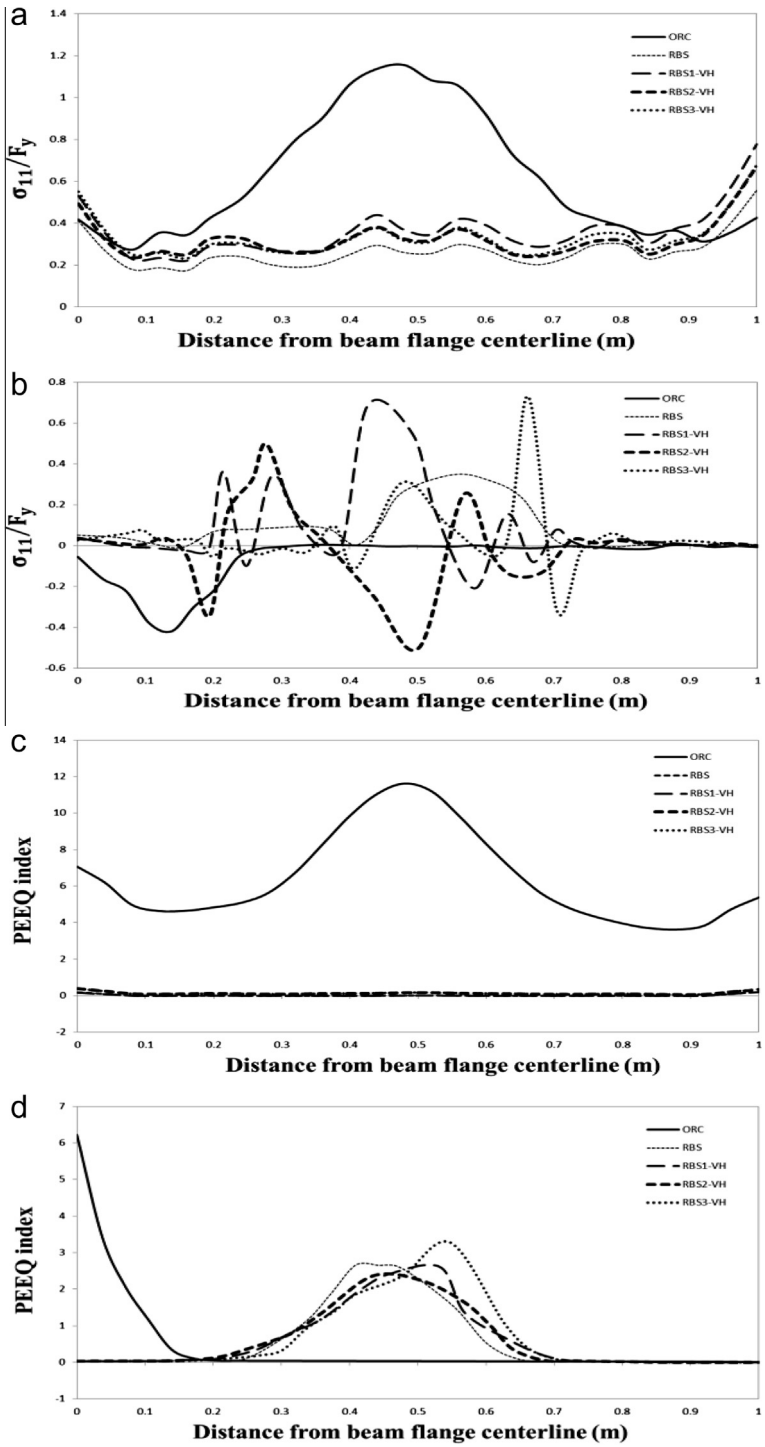

Fig. 12. Longitudinal stresses and PEEQ indices at 0.06 rad rotation for ORC, RBS and RBS-VH: (a) longitudinal stresses along Line A; (b) longitudinal stresses along Line B; (c) PEEQ indices along Line A; (d) PEEQ indices along Line B.

Stress and strain concentrated

The results of finite element analyses are presented in the forms of the normalized longitudinal stress and PEEQ index. The longitudinal stress σ_{11}, represents the normal stress in the beam flange and is normalized by the yield stress F_y of the beam material. As described earlier, the PEEQ index is defined as the plastic equivalent strain (PEEQ) divided by the yield strain ε_y of the beam material, which represents local strain demand [9].

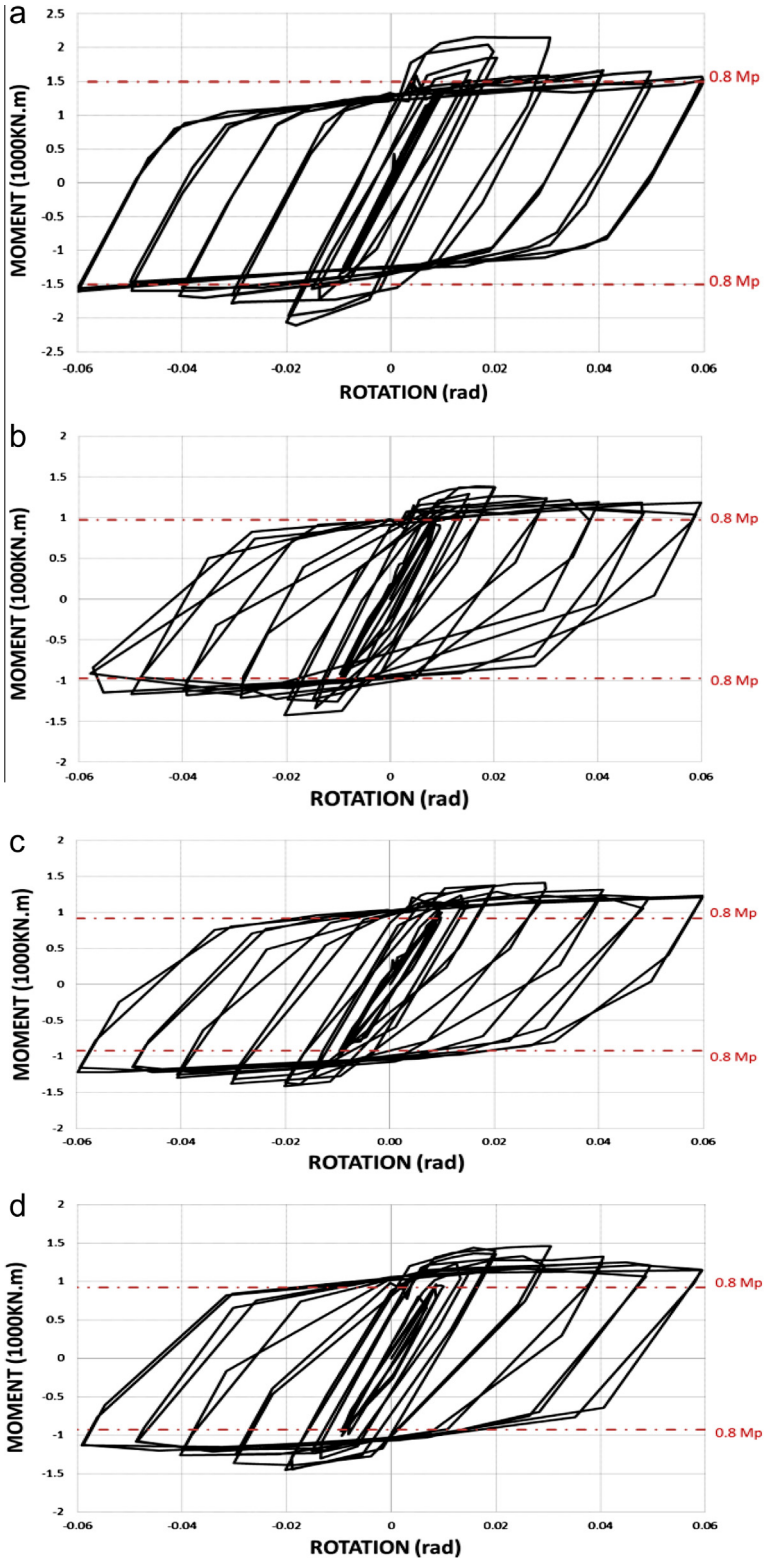

Fig. 13. Histersis response of beam (a) ORC, (b) RBS, (c) RBS1-SH, (d) RBS2-SH, (e) RBS3-SH, (f) RBS1-VH, (g) RBS2-VH, (h) RBS3-VH.

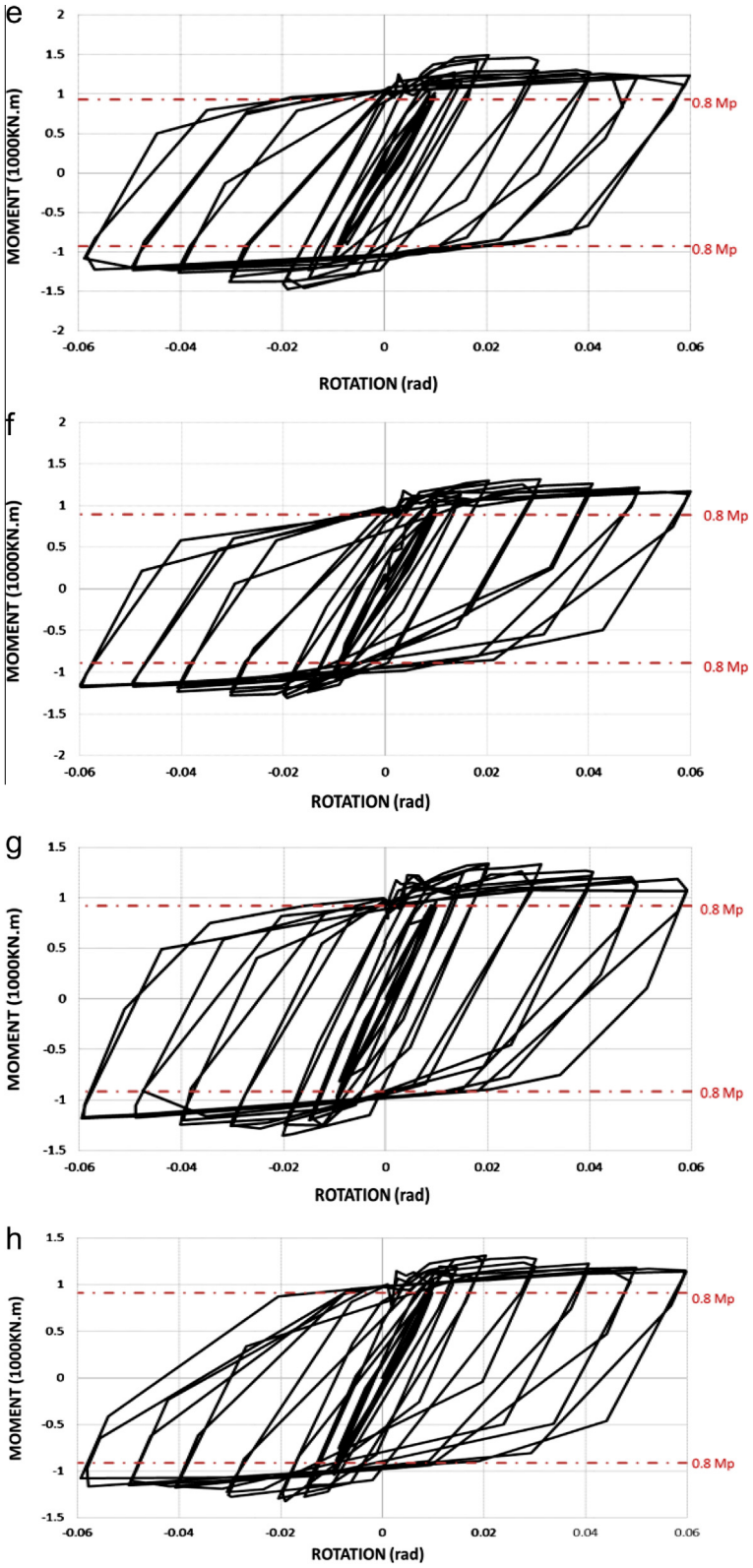

Fig. 13 (*continued*)

Table 3
Stiffness classification of connections.

Models	M_S kN.m	θ_S Rad	K_S kN.m	I m^4	L m	K_SL/EI
ORC	158	0.00134	117,900	197.5e−6	7.6	21.6
RBS	97	0.00112	86,607	121.2e−6	7.6	25.86
RBS1-SH	86	0.00113	76,106	108.5e−6	7.6	25.5
RBS2-SH	92	0.00113	81,311	114.8e−6	7.6	25.62
RBS3-SH	97	0.00112	86,607	121.2e−6	7.6	25.86
RBS1-VH	68	0.00105	64,761	84.34e−6	7.6	27.36
RBS2-VH	78	0.00105	74,285	97.19e−6	7.6	27.76
RBS3-VH	72	0.00105	68,571	90.13e−6	7.6	27.4

The stress and plastic equivalent strain (PEEQ) distributions in two critical sections of the connection were studied. The selection of critical sections was based on the fracturing location in pre-Northridge moment connections. Fig. 10 shows the critical sections, presented by lines running across the width of the beam flange. Line A is located at the complete joint penetration groove weld joining the beam and column flanges because many fractures have been found at this groove weld during the Northridge earthquake. Line B is located at the length of beam flange because that is the main purpose to translate concentrated stress and strain to from connection to beam. Figs. 11a and 12a show that the maximum normal stress divide yield stress on line A for ordinary rigid connection (ORC), RBS connections with same holes (RBS-SH) and RBS connection with varied holes (RBS-VH) are 1.2, 0.42 and 0.4, respectively. Also Figs. 11c and 12c show that PEEQ index for RBS connections and ORC are zero and 12, respectively. As indicate in Figs. 11d and 12d, the PEEQ index are not only zero on surface between beam and column but also take on beam for all types of RBS connection. As it can be seen in Figs. 11 and 12, just for ORC connection the magnitude of normal stress on weld area is greater than yield stress. This result shows that plastic hinge occurred in the connection.

Cyclic behavior

Moment-plastic rotation hysteretic responses of all models are shown in Fig. 13. The moment was measured at the column face and the total beam rotation was computed by dividing the total beam tip displacement by the distance to the column face.

As it can be observed, all models have suitable hysteretic behavior. Hysteretic curves show that the strength of the connection is reduced due to beam local buckling. However, this strength degradation is not so important, since after the buckling, the strength of connection in all models is still more than plastic moment capacity of beams. Therefore, this connection can be classified as a full strength connection. As it can be observed from the hysteretic curves, all models have reached to 0.04 rad rotation, and the strength of connection at 0.04 rad rotation is more than 80% of the beam plastic moment capacity, (0.8 Mp). Consequently, this connection satisfies the criteria of AISC Seismic Provisions (2005) [11] for special moment frame systems. As indicate in Fig. 13a the strength of ORC decrease suddenly after 0.03 rad rotation but all types of RBS connections have slow slip decreasing strength.

Connection stiffness classification

The connections could be classified using moment-joint rotation curves. The joint rotation is considered as the summation of connection rotation and panel zone rotation.

Secant stiffness is computed using moment-joint rotation curves of models. Secant stiffness is defined as:

$$K_S = M_S/\theta_S$$

$$M_S = F_y \times S$$

Where F_y is the yield stress of steel, and S is beam section modulus.

θ_s = joint rotation corresponding to M_S obtained from moment-joint rotation curves.

According to AISC Specifications for Structural Steel Buildings (2005) [11], if $K\,L/EI > 20$ the connections can be considered as fully restrained. Where, L and EI are length and bending rigidity of the beam respectively. Values of secant stiffness and $K\,L/EI$ are presented in Table 3 for all models. The value of L in this table is considered as equal to the length of beam in the frame between two columns which is twice the beam length in each side of column in selected subassemblies.

As it can be seen in Table 3, all models are full restrained connection and also Secant stiffness magnitude in RBS-VH connections is bigger than that in other connections (Fig. 14).

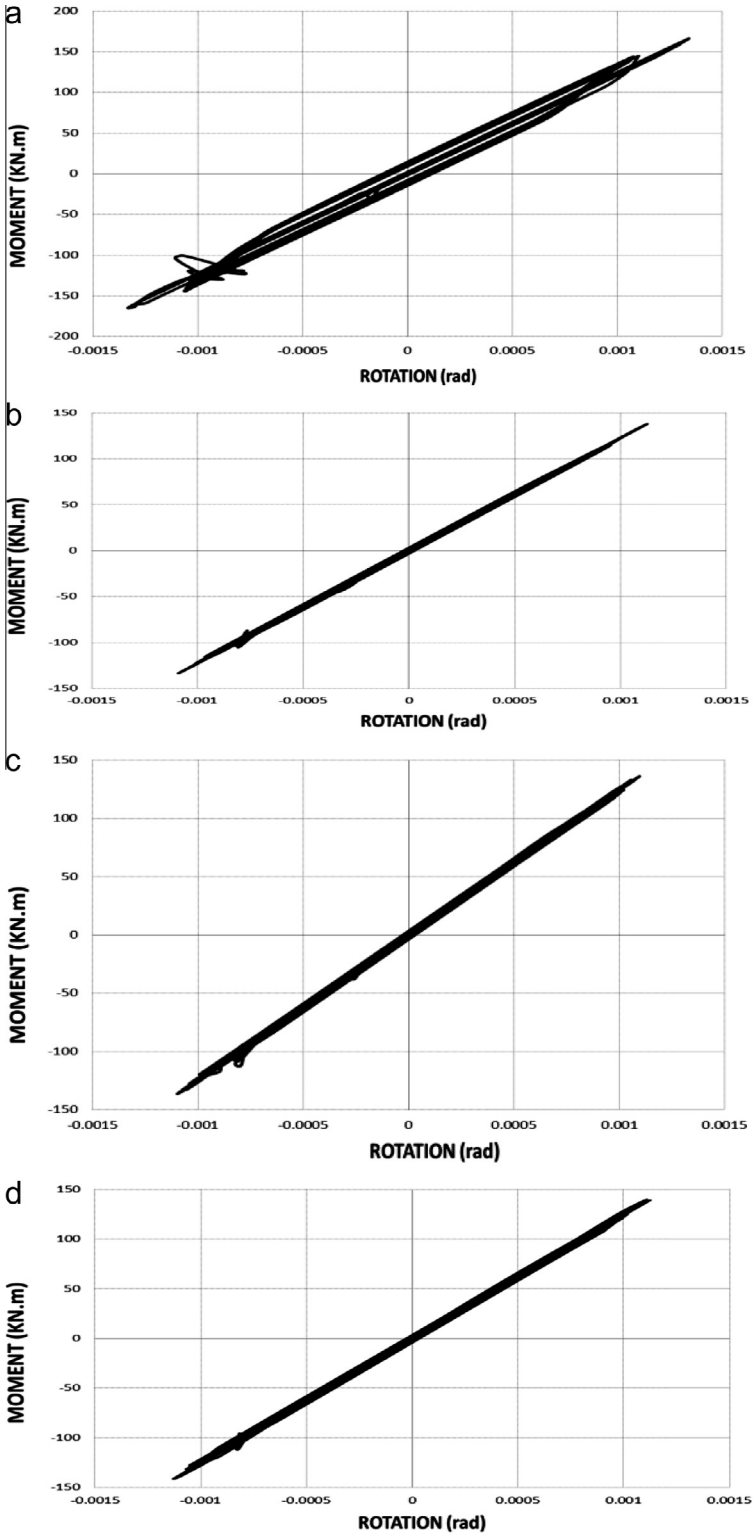

Fig. 14. Histersis response of Panel Zone (a) ORC, (b) RBS, (c) RBS1-SH, (d) RBS2-SH, (e) RBS3-SH, (f) RBS1-VH, (g) RBS2-VH, (h) RBS3-VH.

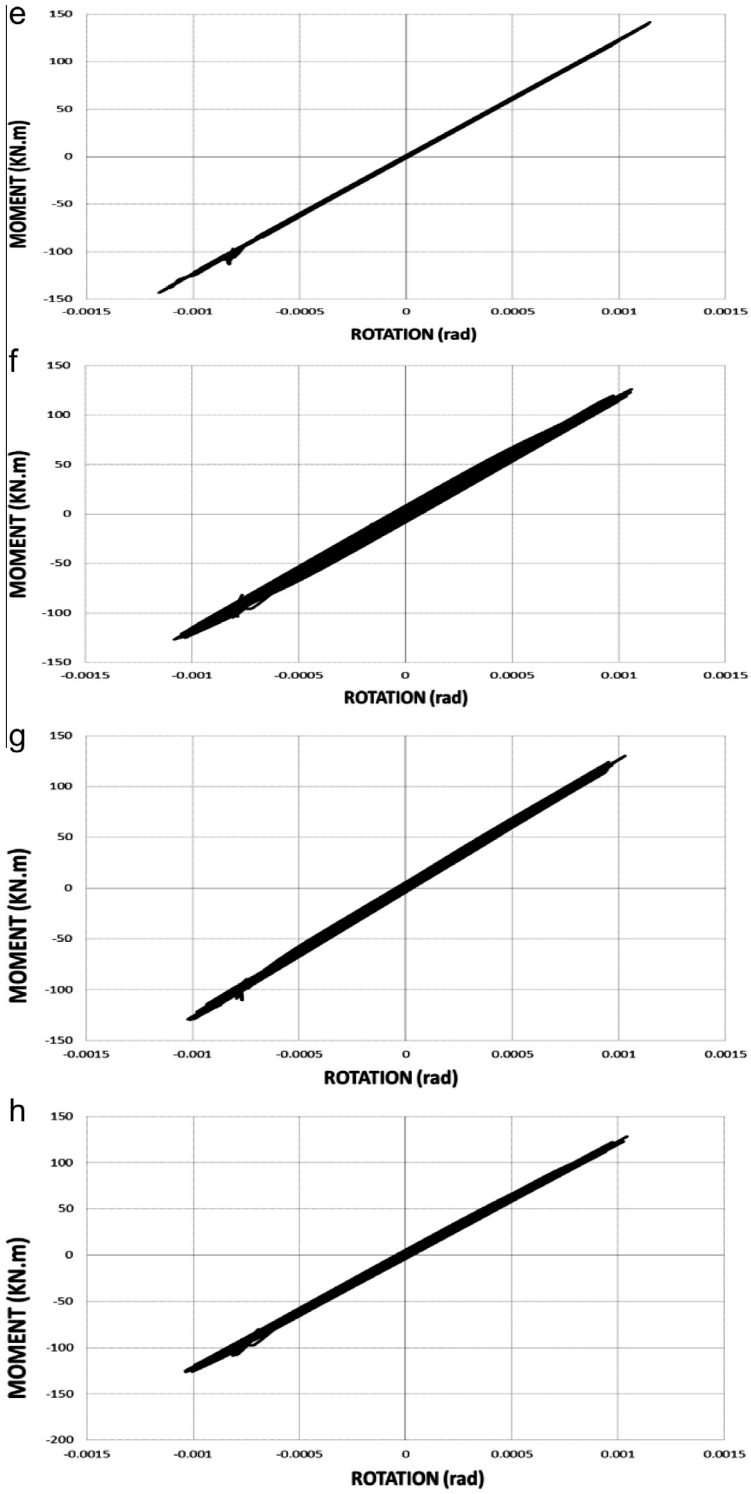

Fig. 14 (*continued*)

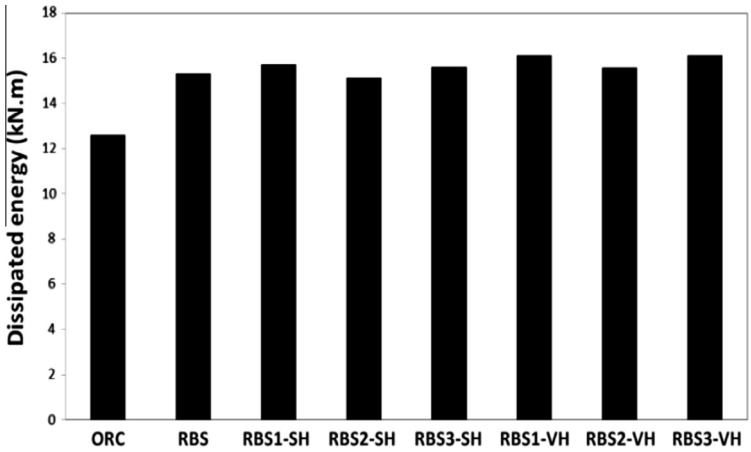

Fig. 15. Energy dissipated by the whole specimen.

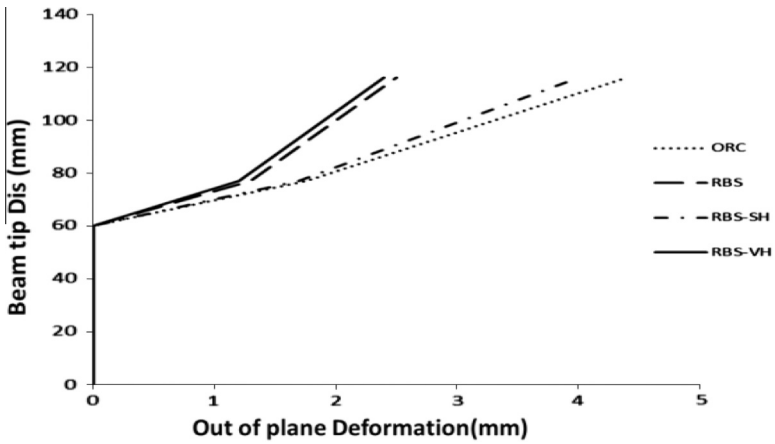

Fig. 16. Buckling behavior of the exterior specimens.

Dissipated energy

The total energy dissipated by each specimen during a complete excursion of 0.06-rad total rotation is illustrated in Fig. 15. The specimens RBS1-VM and RBS3-VM showed a slightly more energy dissipation capability compared to other reduced beam section moment connections. As observed in Fig. 15, reduced beam section increases 18% of dissipated energy.

Out-of-plane deformation due to buckling

The maximum out-of-plane deformation of the beam was determined during the loading. The resulting curves for four specimens are shown in Fig. 16. The buckling onset is recognized from where the curve slope is suddenly degraded. As observed, the tip displacements corresponding to the buckling onset are around 60 mm for all the models and the RBS-VH has minimum buckling to compared to other models.

Conclusions

In this paper, the results obtained from modeling by ABAQUS computer program were provided:

(1) In the RBS connection with the same holes and varied holes, plastic deformations take place significantly in the beam.
(2) Due to using reduced beam section moment connection, the panel zone in all models remains elastic.
(3) As shown in hysteretic curves, this connection is a full strength connection.
(4) This connection can be used in special moment frame (SMF) systems.

(5) Due to using reduced beam section, in moment connection, panel zone rotation is approximately 2–3% of the total rotation; therefore, rotational behavior is completely independent of panel zone participation.
(6) All values of KL/EI are greater than 20; therefore, this type of connection is a fully restrained connection.
(7) Reduced beam section using varied holes, dissipate energy more than other types of reduction and also has minimum magnitude of out of plane buckling.

References

[1] Engelhardt MD, Husain AS. Cyclic-loading performance of welded flange-bolted web connection. J Struct Eng 1993;119.
[2] Engelhardt MD, Winnebeger T, Zekany AJ, Potyaraj TJ. The dog bone connection: part 2. Mod Steel Constr 1996.
[3] Deylami, A. Moslehi Tabar. Experimental study on the key issues affecting cyclic behavior of reduce beam section moment connection. Beijing, China; 2008.
[4] Sang WH, Ki-Hoon M, Stojadinovic B. Design equations for moment strength of RBS-B connections. J Constr Steel Res 2009;65:1087–95.
[5] Sang WH, Ki-Hoon M, Young Seo A, Estimation of rotation capacities of RBS-B connections. In: Proceedings of the 8th ISAIA, Nov. 9–12, 2010. Kitakyushu, Japan; 2010.
[6] Rahnavard R, Siahpolo N. Analytical study on reduce beam section bolt moment connection effecting cyclic behavior. Esfahan, Iran; 2013 (in Persian).
[7] Moslehi Tabar A, Deylami A. Promotion of cyclic behavior of reduced beam section connections restraining beam web to local buckling. Thin Walled Struct 2013;73:112–20.
[8] Chou CC, Lai YJ. Seismic rehabilitation of welded steel beam-to-box column connections utilizing internal flange stiffeners. Earthquake spectra, vol. 26. Earthquake Engineering Research Institute; 2010. p. 927–50. No. 4.
[9] Chen CC, Chen S Wei, Chung M, Lin MC. Cyclic behavior of unreinforced and rib-reinforced moment connections. J Constr Steel Res 2005;61:1–21.
[10] Hancock JW, MacKenzie AC. On the mechanisms of ductile failure in high-strength steels subjected to multi-axial stress-states. J Mech Phys Solids 1976;24:147–69.
[11] Seismic provision for structural steel building. American Institute of Steel Construction, Chicago, Illinois; 2005.
[16] ABAQUS user's manual version 12.

Further reading

[12] Zehang Xiaofeng, Ricles James M, Lu Le-Wu, Fisher John W. Analytical and experimental studies on seismic behavior of deep column-to-beam welded reduced beam section moment connections, 13. Canada: WCC; 2004.
[13] Roeder CW. Connection performance state of art report. Report No. FEMA-335D, Washington, DC; 2000.
[14] Structural welding code-steel, AWS D1.1/D1.1M. Miami, Florida: American Welding Society; 2002.
[15] El-Tawil S, Mikesell T, Kunnath SK. Effect of local details and yield ratio on behavior of FR steel connections. J Struct Eng ASCE 2000;126(1):79–87.